The Astrophysical Journal Letters, 821:L15 (5pp), 2016 April 10 doi:10.3847/2041-8205/821/1/L15

THE NEAREST ISOLATED MEMBER OF THE TW HYDRAE ASSOCIATION IS A GIANT PLANET ANALOG

Kendra Kellogg[1], Stanimir Metchev[1,2], Jonathan Gagné[3,5], and Jacqueline Faherty[3,4,6]
[1] The University of Western Ontario, Centre for Planetary and Space Exploration, Department of Physics & Astronomy, 1151 Richmond Street, London, ON N6A 3K7, Canada; kkellogg@uwo.ca
[2] Stony Brook University, Department of Physics & Astronomy, 100 Nicolls Road, Stony Brook, NY 11794-3800, USA
[3] Carnegie Institution of Washington DTM, 5241 Broad Branch Road NW, Washington, DC 20015, USA
[4] Department of Astrophysics, American Museum of Natural History, Central Park West at 79th Street, New York, NY 10034, USA
Received 2016 February 25; accepted 2016 March 24; published 2016 April 11

ABSTRACT

In a recent search for unusually red L and T dwarfs, we identified 2MASS J11193254–1137466 as a likely young L7 dwarf and potential member of the TW Hydrae association. We present spectra that confirm the youth of this object. We also measure a radial velocity of 8.5 ± 3.3 km s^{-1} that, together with the sky position, proper motion, and photometric distance, results in a 92% probability of membership in the TW Hydrae association, with a calibrated field contamination probability of 0.0005% using the BANYAN II tool. Using the age of TW Hydrae and the luminosity of 2MASS J11193254–1137466, we estimate its mass to be 4.3–7.6 $M_{\rm Jup}$. It is the lowest-mass and nearest isolated member of TW Hydrae at a kinematic distance of 28.9 ± 3.6 pc, and the second-brightest isolated $<10\,M_{\rm Jup}$ object discovered to date.

Key words: brown dwarfs – open clusters and associations: individual (TW Hydrae) – stars: individual (2MASS J11193254–1137466) – techniques: radial velocities

1. INTRODUCTION

Young brown dwarfs, especially at the latest spectral types, have masses and atmospheres similar to those of directly imaged gas giant exoplanets. Isolated young brown dwarfs offer a way to study cool, low-pressure atmospheres of exoplanets without the inherent difficulties of isolating the planet flux from that of a brighter host star. Most of the known isolated planetary-mass brown dwarfs have been found through their unusually red optical and near-infrared colors, often in the regions of young stellar associations (e.g., Luhman et al. 2005; Marsh et al. 2010; Aller et al. 2013; Liu et al. 2013; Schneider et al. 2014). Over the past few years, targeted searches have also encompassed the position–velocity phase spaces of nearby young stellar associations (e.g., Gagné et al. 2014b, 2015c, 2015b), most notably with the Bayesian Analysis for Nearby Young AssociatioNs (BANYAN) tool (Malo et al. 2013). These have helped researchers to recognize or discover the lowest-mass isolated brown dwarfs in the solar neighborhood (Delorme et al. 2012; Liu et al. 2013; Gagné et al. 2014a, 2015a).

In Kellogg et al. (2015) we conducted a comprehensive program to purposefully seek L and T dwarfs with unusual optical/infrared colors in the combined set of SDSS, 2MASS, and *WISE* data. We did not impose positional or space velocity constraints, in order to obtain an unbiased assessment of ultracool dwarfs with peculiar spectral energy distributions (SEDs). One of the newly discovered objects was the extremely red ($J - K_s = 2.58 \pm 0.03$ mag) L7 candidate low-gravity dwarf 2MASS J11193254−1137466 (henceforth, 2MASS J1119–1137). At $K_s = 14.75 \pm 0.01$ mag in the VISTA Hemisphere Survey (VHS; PI McMahon, Cambridge, UK), a confirmation of its youth would place it among the brightest isolated planetary-mass objects, making it exceptionally suitable for investigating exoplanetary atmospheres in detail.

Here we report the spectroscopic confirmation of the low surface gravity of 2MASS J1119–1137, its kinematic association with the TW Hydrae association (TWA; Webb et al. 1999), and hence its planetary mass.

2. OBSERVATIONS AND DATA REDUCTION

To confirm the youth of 2MASS J1119–1137, we obtained low-resolution spectra with FLAMINGOS-2 (Eikenberry et al. 2004) on the Gemini-South telescope through Fast Turnaround program GS-2015B-FT-5. The spectrum revealed weaker gravity-sensitive K I absorption lines than in a typical field-age late-L dwarf, indicating that 2MASS J1119–1137 is young (e.g., Cruz et al. 2009; Rice et al. 2010). Because of unresolved spectrophotometric systematics, namely an extremely red spectral slope and unexpectedly deep OH absorption bands inconsistent with our SpeX spectrum (Kellogg et al. 2015), we do not present the F-2 spectrum here. We subsequently obtained an $R \sim 6000$, 0.8–2.45 μm spectrum with the Folded-port InfraRed Echellette (FIRE; Simcoe et al. 2008, 2013) at the Magellan Baade telescope on 2016 January 21. It is this spectrum that we use for the surface gravity and radial velocity analysis presented herein. We observed the target at the parallactic angle (PA) $\sim 226°$, at an airmass of 1.17–1.05 with good weather conditions and a seeing of $\sim 0\farcs5$. The echelle disperser was used in conjunction with the Sample Up the Ramp (SUTR) readout and high-gain (1.3 e-/DN) modes. A single 900 s exposure and six 600 s exposures were obtained for a total integration time of 1.25 hr, which yielded signal-to-noise ratios of ∼10–70 per pixel in the 1.1–2.2 μm range. We observed the A0 standard HD 85056 immediately afterwards at a similar airmass (1.08–1.09).

We used ThAr calibration lamps (10 s exposure times), observed in the middle and at the end of the science sequence, and again after the telluric standard, to ensure a proper wavelength calibration. A total of 11 internal high-signal flats (1 s exposures with high-voltage lamps) and 11 low-signal flats (10 s exposures with low-voltage lamps) were obtained at the

[5] NASA Sagan Fellow.
[6] Hubble Fellow.

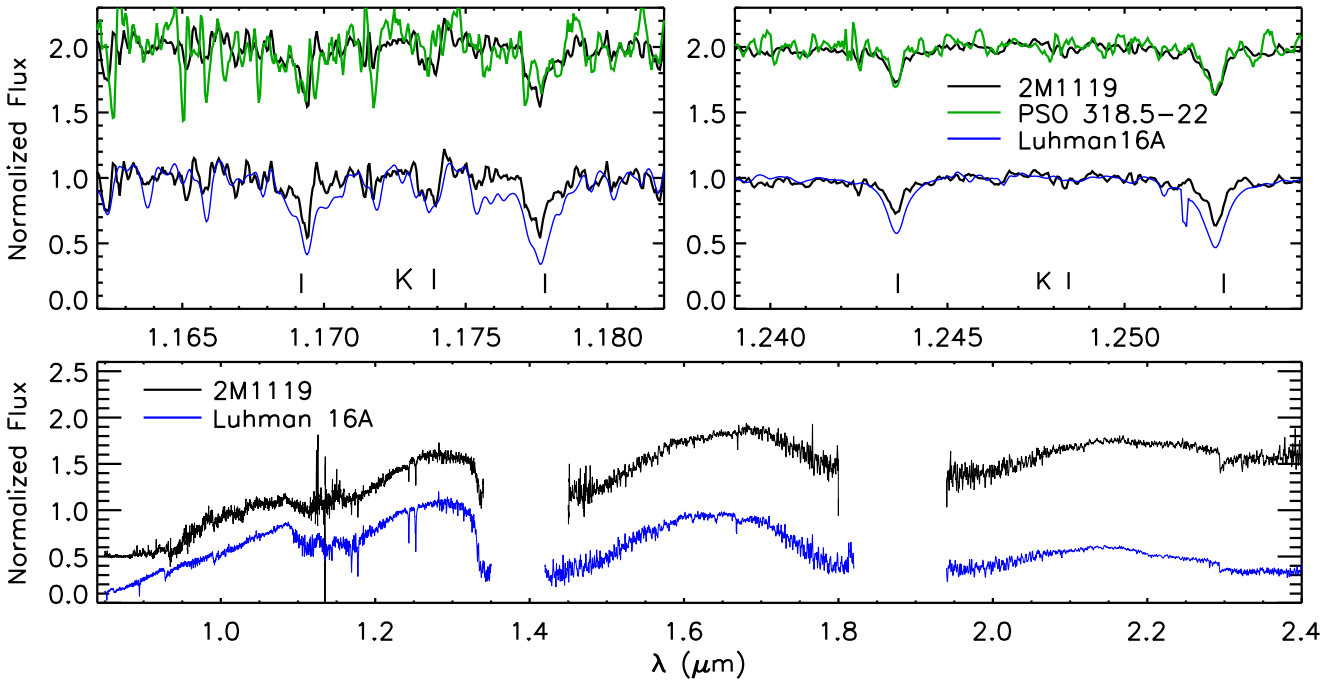

Figure 1. Comparison of the $R \sim 6000$ FIRE spectra of 2MASS J1119–1137 (black), the young L7 dwarf PSO J318.5−22 (green; Faherty et al. 2016), and the old L7.5 dwarf Luhman 16A (blue; Faherty et al. 2014). Top: comparison of the two K I doublet FIRE orders, showing that 2MASS J1119–1137 and PSO J318.5−22 have comparably low surface gravities. Bottom: full FIRE spectra, normalized to unity between 1.25 and 1.30 μm and offset vertically by 0.5 units for clarity. The $\lambda < 1.1$ μm region in the spectrum of 2MASS J1119–1137 has low SNR and the FIRE order stitching is unreliable. The high-order continuum change at 1.55 μm and the CO band head at 2.30 μm fall at FIRE order boundaries, so the strength of these features is also unreliable. The complete spectrum of PSO J318.5−22 (not shown) is presented in Faherty et al. (2016).

beginning of the night: high-signal flats provide a good pixel response calibration in the blue orders, whereas low-signal flats are used for the red orders. Five 4 s dome flats were also obtained to characterize the slit illumination function.

We reduced the data using the Interactive Data Language (IDL) pipeline FIREHOSE, which is based on the MASE (Bochanski et al. 2009) and SpeXTool (Vacca et al. 2003; Cushing et al. 2004) packages. The pipeline was modified to achieve a better rejection of bad pixels (i.e., see Gagné et al. 2015b, 2015d[7]). This reduction package includes a barycentric velocity correction and converts the wavelength solution to vacuum.

3. CONFIRMATION OF YOUTH

To determine if 2MASS J1119–1137 is young, we focused our analysis on the gravity-sensitive K I absorption lines (1.1692 and 1.1778 μm, 1.2437 and 1.2529 μm). Our FIRE spectrum has 40 times the resolution of our previous SpeX prism spectrum (Kellogg et al. 2015), allowing us to directly compare the strength of the spectral features to those of young and field-age late-L dwarfs. The top panels of Figure 1 show sections of our FIRE spectrum (black) compared to FIRE spectra of the young L7 dwarf PSO J318.5338−22.8603 (green; hereafter PSO J318.5−22; Faherty et al. 2016) and the field-aged L7.5 dwarf Luhman 16A (blue; Faherty et al. 2014) centered on the K I lines. The K I lines in the 2MASS J1119–1137 spectrum are weaker than in Luhman 16A, indicating low surface gravity and hence a young age ($\lesssim$200 Myr; Allers & Liu 2013). Conversely, the K I line strengths of 2MASS J1119–1137 and PSO J318.5−22 are indistinguishable from each other. The two objects are among the reddest isolated L dwarfs known to date. The equivalent widths of the K I lines as defined by McLean et al. (2003) for 2MASS J1119–1137 (1.21 ± 0.66 Å at 1.1168 μm; 3.84 ± 0.64 Å at 1.1177 μm; 1.89 ± 0.29 Å at 1.1243 μm; and 3.12 ± 0.31 Å at 1.1254 μm) are systematically lower than those of field L7 dwarfs (e.g., see McLean et al. 2003, Figure 15). The complete $R \sim 6000$, 0.7−2.4 μm FIRE spectrum of 2MASS J1119–1137 is shown in the bottom panel of Figure 1, where it is seen to be significantly redder than the near-IR spectrum of the field-aged L7.5 dwarf Luhman 16A.

The combined evidence leads us to conclude that 2MASS J1119–1137 is indeed young, and is comparable in age to the 23 Myr old β Pictoris association member PSO J318.5−22. At the current signal-to-noise ratios and resolutions, we cannot determine if one object is younger than the other from the spectra alone. From this comparison, together with the very red color and the consistency of various spectral features and indices with other young, late-L dwarfs (Kellogg et al. 2015), we conclude that 2MASS J1119–1137 has low surface gravity and is likely $\lesssim$120 Myr old.

4. KINEMATICS

We used single-exposure, single-order, and telluric-corrected FIRE spectra to measure the radial velocity of 2MASS J1119–1137. We used a forward modeling approach that relies on the zero-velocity BT-Settl atmosphere models (Baraffe et al. 2003; Allard et al. 2013) to reproduce our observations. Our forward model employs four free parameters: a radial velocity shift, an instrumental line spread function (LSF) width where the LSF is modeled as a Gaussian function,

[7] The modified FireHose 2.0 data reduction package can be found at https://github.com/jgagneastro/FireHose_v2/tree/v2.0.

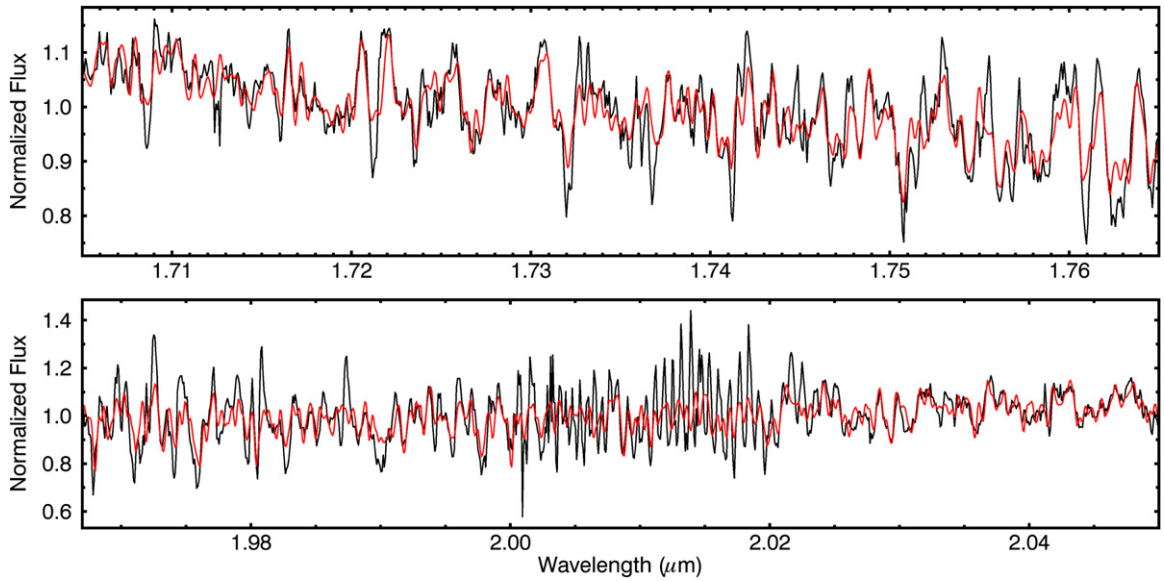

Figure 2. Forward model fitting (red line) to the observed spectra (black line) in echelle orders 15 and 13, in order to determine the radial velocity of 2MASS J1119–1137.

and a two-parameter linear slope multiplicative correction to account for instrumental effects.

We used the IDL implementation of AMOEBA to identify the set of parameters that minimize the reduced χ^2 between the forward model and the observed spectrum. This is similar to the algorithm described by Allers et al. (2016), except that telluric absorption was corrected a priori and we did not attempt to measure $v \sin i$ with the limited resolution of our data. This optimization was carried out on the seven individual exposures, in a selected set of wavelength ranges that are located away from order boundaries and in regions where the S/N is high and sufficient radial velocity information is present in the science spectrum. We selected specific wavelength regions in orders 24 (1.092–1.120 μm), 17 (1.510–1.554 μm), 15 (1.680–1.790 μm), and 13 (1.960–2.050 μm) that satisfied these criteria. We used the BT-Settl model with $T_{\rm eff} = 1600$ K and $\log g = 4.0$, which yielded the smallest reduced χ^2 in these orders with no velocity shift. This temperature and surface gravity are in agreement with those found for PSO J318.5−22 (Liu et al. 2013). We display two example model fits that we obtained in Figure 2.

In each order, the useful wavelength range was split into 15 individual segments of width 0.02 μm to account for sub-pixel systematic effects in the wavelength calibration (e.g., see Gagné et al. 2015a). This yielded a total of 420 individual radial velocity measurements (7 exposures, 4 orders, and 15 order segments). The single-exposure radial velocities were first combined at every wavelength range using an SNR-squared weighted mean. A weighted standard deviation was used to obtain measurement errors on each of these radial velocity measurements.

This method yielded a weighted-average radial velocity of 8.5 ± 1.3 km s^{-1}. Similar radial velocity measurements with FIRE have been demonstrated to bear a 3 km s^{-1} systematic uncertainty (e.g., see Zapatero Osorio et al. 2007), which we add in quadrature to our measurement to obtain 8.5 ± 3.3 km s^{-1}.

In order to calibrate our method, we applied it to FIRE data obtained for PSO J318.5−22, for the young T5.5 SDSS J111010.01+011613.1 (Gagné et al. 2015a), and for three young M9.5–L2 brown dwarfs with Keck NIRSPEC radial velocity measurements (2MASS J02340093–6442068, 2MASS J02103857–3015313, 2MASS J23225299–6151275; Faherty et al. 2016). We found measurement discrepancies between 0.5 and 4.4 km s^{-1} with a standard deviation of 1.5 km s^{-1}, well within our measurement errors. These data will be detailed in a future publication.

We solved for the proper motion from the 14-year baseline spanned by 2MASS, SDSS, *WISE*, *WISE* 3-Band Post-Cryo, and *NEOWISE*-R images, using relative astrometry as prescribed in Kirkpatrick et al. (2014). The total proper motion differs slightly from the measurement in Kellogg et al. (2015), which was obtained only from the difference between the 2MASS and AllWISE positions.

5. TWA MEMBERSHIP

We used our radial velocity measurement, along with the sky position and proper motion of 2MASS J1119–1137 (Table 1), to calculate a young moving group membership probability with the BANYAN II tool[8] (Gagné et al. 2014b). The BANYAN II tool assumes Gaussian ellipsoid models adjusted to fit the *XYZ* and *UVW* distributions of known bona fide members of different moving groups, or the Besançon galactic model (Robin et al. 2012) for the field hypothesis. Bayes theorem is used to derive a probability density from the comparison of the measurements to the models, and the probability is obtained by marginalizing the probability density function over all possible distances.

We obtained an 88% probability that 2MASS J1119–1137 is a TWA member, with a calibrated field contamination probability of 0.003%, equivalent to a statistical significance of 4.15σ. The coordinate that puts the most stringent constraint on the membership of 2MASS J1119–1137 is *Z*, which only matches the distribution of TWA members. The statistical kinematic distance is 28.9 ± 3.6 pc, consistent with our earlier

[8] Publicly available at http://www.astro.umontreal.ca/-gagne/banyanII.php.

Table 1
Characteristics of 2MASS J11193254–1137466

R.A.	$11^h19^m32^s.543$
decl.	$-11°37'46''.70$
Radial Velocity	8.5 ± 3.3 km s^{-1}
$\mu_\alpha \cos\delta$	-145.1 ± 14.9 mas yr^{-1}
μ_δ	-72.4 ± 16.0 mas yr^{-1}
Y	19.045 ± 0.093 mag
J	17.330 ± 0.029 mag
H	15.844 ± 0.017 mag
K_s	14.751 ± 0.012 mag
$W1$	13.548 ± 0.026 mag
$W2$	12.883 ± 0.027 mag
log $L/L_\odot$	-4.39 ± 0.14
Age	10 ± 3 Myr
Kinematic Distance	28.9 ± 3.6 pc
Estimated Mass	4.3–7.6 $M_{\rm Jup}$

Note. $YJHK_s$ magnitudes from the VHS. http://www.vista-vhs.org/.

photometric estimate of 27 ± 7.2 pc (Kellogg et al. 2015), which was calculated from the apparent K_s magnitude and the expected absolute K_s magnitude of a young L7 dwarf (Filippazzo et al. 2015). The distance is also consistent with the absolute magnitude relations for other young, late-type L dwarfs (e.g., WISEP J004701.06+680352.1 and PSO J318.5 −22; Faherty et al. 2016), which take into account all young L dwarfs. When we include the photometric distance estimate as an input to the BANYAN II algorithm, the TWA membership probability increases to 92% and the field contamination probability significantly decreases to 0.0005%, meaning that 2MASS J1119–1137 is consistent with being a TWA member at a statistical significance of 4.55σ.

In Figure 3 we display the galactic position XYZ and space velocity UVW of 2MASS J1119–1137 at its statistical distance, compared to known bona fide TWA members, and to the 1σ contours of the 3D Gaussian ellipsoid models used in BANYAN II. Although the current model of TWA extends its 1σ contour to only ∼33 pc, this ∼25 pc object appears to have been drawn from the same Gaussian random distribution in $XYZUVW$ space. The XYZ position of 2MASS J1119–1137 reveals it to be the nearest TWA member and extends the observed distance distribution of currently known objects. While other closer candidate TWA members have been reported in the literature (TWA 22; Song et al. 2003), their space positions and velocities fall well outside of the TWA ellipsoid (Mamajek 2005; Teixeira et al. 2009; Weinberger et al. 2013). Our own calculation with BANYAN II yields an association probability of 10^{-7} for TWA 22.

At the age of TWA (10 ± 3 Myr; Bell et al. 2015), we estimate that the mass of 2MASS J1119–1137 is 4.3–7.6 $M_{\rm Jup}$, where we have compared the bolometric luminosity derived from the K_s magnitude at its TW Hydrae kinematic distance and age to model predictions from Saumon & Marley (2008) and directly compared the absolute K_s magnitude to the predictions from Baraffe et al. (2015).

The mass makes 2MASS J1119–1137 comparable to the early-L companion object, 2M1207b (Chauvin et al. 2004, 2005), which is also a member of TW Hydrae (Gizis 2002). The two objects have similar $H - K_s$ colors (1.16 ± 0.24 mag for 2M1207b; Chauvin et al. 2004) to within the uncertainties, although 2M1207b is overall redder in the 1–4 μm region (Chauvin et al. 2004; Song et al. 2006). The

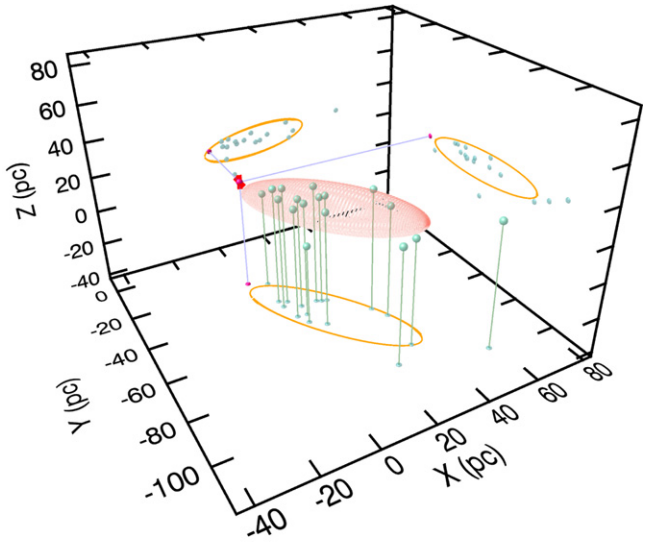

(a) XYZ galactic position

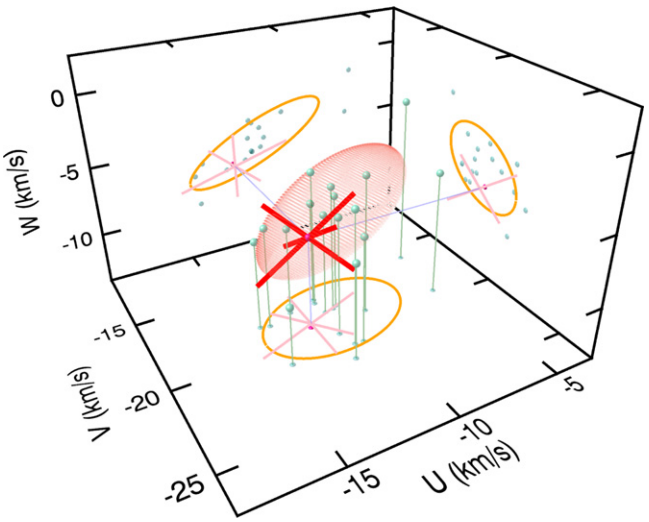

(b) UVW space velocity

Figure 3. Galactic position and space velocity of 2MASS J1119–1137 (red sphere and red error bars) compared to known TW Hydrae bona fide members (green spheres) and the 1σ Gaussian ellipsoid spatial and kinematic models used in BANYAN II (orange ellipses). The data are projected to the three 2D planes for an easier visualization.

0.4 dex lower luminosity of 2M1207b (Filippazzo et al. 2015) reveals that it is likely lower in mass, regardless of model assumptions. Comparing to the cooling tracks of Saumon & Marley (2008) and Baraffe et al. (2015), 2M1207b has an estimated mass of 3.3–5.4 $M_{\rm Jup}$. Our mass estimate for 2MASS J1119–1137 is slightly higher, 4.3–7.6 $M_{\rm Jup}$, which still leaves it as the least massive isolated member of TWA. Both objects are at or above the theoretical opacity-limited turbulent fragmentation limit of 3–5 $M_{\rm Jup}$ (Boyd & Whitworth 2005), so both could have formed through star-like gravo-turbulent collapse. However, both have masses comparable to or smaller than the 5–7 $M_{\rm Jup}$ masses of the HR 8799 planets (Marois et al. 2008, 2010). Hence both 2MASS J1119–1137 and 2M1207b could have in principle

formed, and in the case of 2MASS J1119–1137, subsequently been ejected, via a planet-like mechanism.

We sought bright common proper motion companions to 2MASS J1119–1137 by calculating the 2MASS–AllWISE proper motions of all 2MASS entries within 60′, corresponding to a maximum physical separation of 22,500 au at 25 pc. None of the 368 2MASS sources within this radius had a proper motion within 76 mas yr^{-1} of that of 2MASS J1119–1137, indicating no potential stellar host to this young planetary-mass object.

6. CONCLUSION

We have spectroscopically confirmed the low surface gravity, and hence youth, of the L7 dwarf 2MASS J1119–1137. Its radial velocity, proper motion, and galactic position are consistent with that of the 10 ± 3 Myr old TWA. From the object's near-infrared absolute magnitudes we determine a mass of 4.3–7.6 $M_{\rm Jup}$. It is the nearest member of TWA, and the second-brightest isolated $<10\,M_{\rm Jup}$ object discovered to date. Hence, 2MASS J1119–1137 is an excellent benchmark for young, directly imaged extrasolar planets.

We would like to thank our anonymous referee for their helpful comments. We thank Adam Burgasser and Katelyn Allers for helpful comments with respect to the radial velocity measurement method. We thank Robert Simcoe for help with the data reduction. This work was supported by an NSERC Discovery grant to S.M. at the University of Western Ontario. This work was performed in part under contract with the California Institute of Technology (Caltech)/Jet Propulsion Laboratory (JPL) funded by NASA through the Sagan Fellowship Program executed by the NASA Exoplanet Science Institute. This paper includes data gathered with the 6.5 m Magellan Telescopes located at Las Campanas Observatory, Chile.

Facilities: Gemini-South (Flamingos-2), Magellan: Baade (FIRE).

Software: IDL, FIREHOSE, IRAF.

REFERENCES

Allard, F., Homeier, D., Freytag, B., Schaffenberger, W., & Rajpurohit, A. S. 2013, MmSAI, 24, 128
Aller, K. M., Kraus, A. L., Liu, M. C., et al. 2013, ApJ, 773, 63
Allers, K. N., Gallimore, J. F., Liu, M. C., & Dupuy, T. J. 2016, ApJ, 819, 133
Allers, K. N., & Liu, M. C. 2013, ApJ, 772, 79
Baraffe, I., Chabrier, G., Barman, T. S., Allard, F., & Hauschildt, P. H. 2003, A&A, 402, 701
Baraffe, I., Homeier, D., Allard, F., & Chabrier, G. 2015, A&A, 577, A42
Bell, C. P. M., Mamajek, E. E., & Naylor, T. 2015, MNRAS, 454, 593
Bochanski, J. J., Hennawi, J. F., Simcoe, R. A., et al. 2009, PASP, 121, 1409
Boyd, D. F. A., & Whitworth, A. P. 2005, A&A, 430, 1059
Chauvin, G., Lagrange, A.-M., Dumas, C., et al. 2004, A&A, 425, L29
Chauvin, G., Lagrange, A.-M., Dumas, C., et al. 2005, A&A, 438, L25
Cruz, K. L., Kirkpatrick, J. D., & Burgasser, A. J. 2009, AJ, 137, 3345
Cushing, M. C., Vacca, W. D., & Rayner, J. T. 2004, PASP, 116, 362
Delorme, P., Gagné, J., Malo, L., et al. 2012, A&A, 548, A26
Eikenberry, S. S., Elston, R., Raines, S. N., et al. 2004, Proc. SPIE, 5492, 1196
Faherty, J. K., Beletsky, Y., Burgasser, A. J., et al. 2014, ApJ, 790, 90
Faherty, J. K., et al. 2016, ApJ, submitted
Filippazzo, J. C., Rice, E. L., Faherty, J., et al. 2015, ApJ, 810, 158
Gagné, J., Burgasser, A. J., Faherty, J. K., et al. 2015a, ApJL, 808, L20
Gagné, J., Faherty, J. K., Cruz, K. L., et al. 2014a, ApJL, 785, L14
Gagné, J., Faherty, J. K., Cruz, K. L., et al. 2015b, ApJS, 219, 33
Gagné, J., Lafrenière, D., Doyon, R., Malo, L., & Artigau, É 2014b, ApJ, 783, 121
Gagné, J., Lafrenière, D., Doyon, R., Malo, L., & Artigau, É 2015c, ApJ, 798, 73
Gagné, J., Lambrides, E., Faherty, J. K., & Simcoe, R. 2015d, Firehose, v2.0, Zenodo
Gizis, J. E. 2002, ApJ, 575, 484
Kellogg, K., Metchev, S., Geißler, K., et al. 2015, AJ, 150, 182
Kirkpatrick, J. D., Schneider, A., Fajardo-Acosta, S., et al. 2014, ApJ, 783, 122
Liu, M. C., Magnier, E. A., Deacon, N. R., et al. 2013, ApJL, 777, L20
Luhman, K. L., Adame, L., D'Alessio, P., et al. 2005, ApJL, 635, L93
Malo, L., Doyon, R., Lafrenière, D., et al. 2013, ApJ, 762, 88
Mamajek, E. E. 2005, ApJ, 634, 1385
Marois, C., Macintosh, B., Barman, T., et al. 2008, Sci, 322, 1348
Marois, C., Zuckerman, B., Konopacky, Q. M., Macintosh, B., & Barman, T. 2010, Natur, 468, 1080
Marsh, K. A., Kirkpatrick, J. D., & Plavchan, P. 2010, ApJL, 709, L158
McLean, I. S., McGovern, M. R., Burgasser, A. J., et al. 2003, ApJ, 596, 561
Rice, E. L., Barman, T., Mclean, I. S., Prato, L., & Kirkpatrick, J. D. 2010, ApJS, 186, 63
Robin, A. C., Marshall, D. J., Schultheis, M., & Reylé, C. 2012, A&A, 538, A106
Saumon, D., & Marley, M. S. 2008, ApJ, 689, 1327
Schneider, A. C., Cushing, M. C., Kirkpatrick, J. D., et al. 2014, AJ, 147, 34
Simcoe, R. A., Burgasser, A. J., Bernstein, R. A., et al. 2008, Proc. SPIE, 7014, 70140U
Simcoe, R. A., Burgasser, A. J., Schechter, P. L., et al. 2013, PASP, 125, 270
Song, I., Schneider, G., Zuckerman, B., et al. 2006, ApJ, 652, 724
Song, I., Zuckerman, B., & Bessell, M. S. 2003, ApJ, 599, 342
Teixeira, R., Ducourant, C., Chauvin, G., et al. 2009, A&A, 503, 281
Vacca, W. D., Cushing, M. C., & Rayner, J. T. 2003, PASP, 115, 389
Webb, R. A., Zuckerman, B., Platais, I., et al. 1999, ApJL, 512, L63
Weinberger, A. J., Anglada-Escudé, G., & Boss, A. P. 2013, ApJ, 762, 118
Zapatero Osorio, M. R., Martín, E. L., Béjar, V. J. S., et al. 2007, ApJ, 666, 1205